between the methyl group and the glucose skeleton, and a schematic pathway of the Embden-Meyeroff cycle in which all the hydrogen atoms bound to carbon atoms in the sugar would be involved in proton transfers with the fermentation aqueous medium may be excluded. From the redistribution coefficients calculated above, the influence of glucose appears to strongly predominate over that of water. However, since the introduction of hydrogen isotopes issued from water may occur with strong discriminating effects against deuterium, the redistribution coefficients cannot be considered as directly representing the relative numbers of hydrogens derived from the sugar and water materials. More specific information can be advanced on the basis of the large deviations with respect to a statistical distribution, observed in the isotope contents of the different sites of glucose. Thus the strong depletion occurring in the methyl site of ethanol as compared to the overall isotope content of glucose should be put together with the relatively low isotope parameters of the anomeric site and to a lesser extent of the methylene sites 6,6' of glucose. In the hypothesis of similar values of the fractionation factors accompanying the introduction of deuterium atoms from water into the methyl and methylene sites of ethanol, the number of hydrogens n_1^W issued from water and entering the methyl site can be estimated. Thus on the basis of the coefficients $a_{22} \simeq 0.7$ and $a_{12} \simeq 0.23$ deduced from the investigation of $(D/H)_{II}$ and $(D/H)_I$, respectively, a value $n_1^W \simeq 2$ is calculated. In this hypothesis, the glucose skeleton would therefore contribute four hydrogens to the methyl groups of the two ethanol molecules issued from the fermentation of one molecule of glucose, the two remaining hydrogens coming from the water medium.

A priori it could be considered that the strong fractionation effects intervening in the biochemical synthesis of ethanol render its use as a probe for characterizing the starting materials questionable.[15] However, the present results demonstrate that constant redistribution parameters are involved in standardized conditions. From a practical point of view these results therefore legitimate the use of the isotope parameters of the fermentation products as a fingerprint of the parent compounds, i.e., glucose and water. More generally since we have proved that hydrolysis of starch and inversion of sucrose occur without modification of the natural deuterium distribution in the glucose unit of these glucides,[19] the isotope parameters measured in ethanol and water samples issued from the fermentation of the various forms of glucides offer a faithful image of the original natural species and therefore contain invaluable geographical, climatological, and biochemical information. This fingerprint concept is the basis of a powerful tool in the quality control of foods and beverages and in tracer studies of photosynthesis reactions and bioconversion processes.[6]

Acknowledgment. We gratefully acknowledge the gift of Antarctic water (from the French expedition in 1983) by Dr. Lorius (Laboratoire de Glaciologie CNRS, Grenoble).

Registry No. EtOH, 64-17-5; D_2, 7782-39-0; D-glucose, 50-99-7; sucrose, 57-50-1.

Why the Accumulation of Electron Density Appears Weak or Absent in Certain Covalent Bonds†

Kathryn L. Kunze and Michael B. Hall*

Contribution from the Department of Chemistry, Texas A&M University, College Station, Texas 77843. *Received November 13, 1985*

Abstract: The standard deformation density, molecular density minus spherical atom densities, may appear small or even negative in certain covalent bonds. For example, in difluorine subtraction of the electron densities of spherically averaged F atoms, which include all components of the $^2P(2s^22p^5)$ ground state, results in the standard deformation density. Contour maps show an electron density deficit along the bond axis in both the internuclear bonding region and the lone-pair regions beyond the nuclei and accumulation in the π regions perpendicular to that axis. This result resembles experimental maps of the deformation density of the covalent bond between electronegative atoms such as that between the O atoms of peroxides. Our analysis shows that one can interpret this type of deformation density as a combination of constructive interference (covalent bond formation) and atomic reorientation, polarization, promotion, and hybridization (atom preparation for bonding). Subtraction of the electron densities of one component of the ^2P ground state of the F atoms, oriented with singly occupied $2p_z$ orbitals along the σ direction, results in maps with weak accumulation of charge in the bonding region between the nuclei, deep troughs of density deficit near the nuclei, no change along the π regions, and accumulation of charge in the lone-pair regions beyond the nuclear centers. Subtraction of the electron densities of optimally hybridized valence-state F atoms matches the lone-pair densities of atoms and molecule, so that the total difference is dominated by a localized bonding orbital density difference. This map reveals not only the accumulation of charge in the internuclear region but also the concomitant depletion of charge in the nonbonding regions beyond the nuclear centers which together are the signature of the covalent bond. Thus, if one views bond formation in two steps, atom preparation then bond formation, one easily sees the origin of the loss of electron density in the bond region caused when two spherical F atoms form a bond.

Recently, the number of studies of the electron density distribution, $\rho(\vec{r})$, in molecules by means of X-ray diffraction have increased.[1] Part of the interest arises from the promise, given by the theorem of Hohenberg and Kohn,[2] of the existence of a direct relationship between the electron density and the energy of the ground-state molecule. Most experimental studies measure what is called the standard deformation density, $\Delta\rho(\vec{r})$, which is defined as the molecular electron density minus the electron density of the promolecule[3] made up of the superposition of isolated, neutral, spherically averaged, ground-state atoms.

† Presented at the XIIIth Congress and General Assembly of the International Union of Crystallography, August 9-18, 1984, Hamburg, FDR.

(1) Coppens, P.; Hall, M. B., Eds. *Electron Distributions and the Chemical Bond*; Plenum Press: New York, 1982.
(2) Hohenberg, P.; Kohn, W. *Phys. Rev.* **1964**, *B136*, 864.
(3) Hirshfeld, F. L.; Rzotkiewicz, S. *Mol. Phys.* **1974**, *27*, 1319.

0002-7863/86/1508-5122$01.50/0

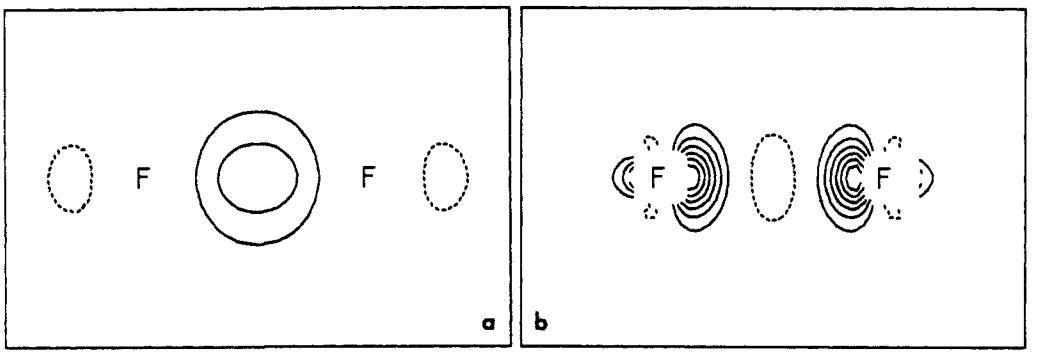

Figure 1. Contour plots of the difference in electron density distribution of the F_2 molecule. (a) Difference in total electron density of the HFR calculation in the triple-ζ plus polarization (TZP) and triple-ζ (TZ) basis sets. (b) Difference in total electron density of the GMO–CI and HFR calculations in the TZP basis. All plots in this paper are in the plane containing the F atoms. Positive contours are solid, negative contours are dashed, and zero contour is omitted. Adjacent contours differ by an increment of 0.1 electron Å^{-3}. The smallest contour is ±0.1 electron Å^{-3}.

Sometimes it is difficult to reconcile an interpretation of the standard deformation density with our usual concepts of bonding. The prototypes for the covalent bond are the bonds of the hydrogen molecule and hydrogen molecule ion,[4,5] where the buildup of electron density in the bonding region between the nuclei and the depletion in the nonbonding region are the signature of covalent bonding. However, numerous experimental and theoretical studies have reported deformation density maps which show density deficits or weak accumulations at or near positions where "bonding density" peaks were expected between formally covalently bonded atoms.[6-11] For example, bonding density deficits are found in the experimental and theoretical maps of the O–O bond in H_2O_2[6,7] and organic peroxides[8] and theoretical maps of the F–F bond in F_2.[7] Weak bonding density accumulations were found in experimental maps for NN, CN, CO, and CF bonds of various organic molecules.[8-11] This has reminded some[8,9a] of the fundamental controversy over the origin of covalent bonding.[3-5,12-14] The results of sophisticated theoretical calculations using reference densities lead Bader et al. and Hirshfeld and Rzotkiewic to stress the atypical nature of the hydrogen molecule and its unsuitability for a general discussion of the covalent bond.[3,13-15] Bader and co-workers analyze the total density directly by examining the Laplacian of the density. However, for F_2 the Laplacian does not reveal the covalent bond.[15]

In this paper, we demonstrate why the electron density in covalent bonds may appear weak or absent and how electron density accumulation and depletion can be revealed in a way which is meaningful for the chemist. We present the theoretical calculation and comparison of several types of maps of the electron-density difference for the covalently bonded fluorine molecule. This molecule is the simplest system that has no accumulation of density in the standard deformation density.

While this paper was being reviewed, Ruedenberg and coworkers published a paper which advanced similar conclusions regarding the question posed in the title.[16]

Computational Procedure

The molecular and atomic orbitals were generated by ab initio calculations using as basis functions the standard Dunning triple-ζ [5s3p] contraction[17a] of the Huzinaga (9s5p) primitive Gaussian basis,[17b] both with and without a set of d polarization functions with exponent 0.90.[18] The experimental equilibrium molecular bond length of 2.68 a.u.[19a] has been used. Orbitals for the molecule were generated by calculations at the single determinant Hartree–Fock–Roothaan (HFR) level.[20] As a further refinement, orbitals for the molecule were generated from the generalized molecular orbital (GMO) method,[21] a limited type of multiconfiguration self-consistent-field (MCSCF) calculation. In the case of difluorine, the configuration interaction (CI) necessary to dissociate the molecule properly consists of the dominant single determinant plus the paired double excitation from this bonding orbital, $3\sigma_g$, to its antibonding counterpart, $3\sigma_u$. The GMO–CI consisted of this two-configuration self-consistent-field calculation. The canonical HFR molecular valence orbitals, which are delocalized over the entire molecule, were localized by using the Boys criteria[22] to generate orbitals for the individual bonding molecular-orbital density and lone-pair molecular-orbital densities. The localization of the molecular orbitals is an orthonormal transformation and does not change the total energy or the total electron density distribution. The atomic hybridization of each LMO was evaluated.[23]

Atomic orbitals were generated by calculations at the symmetry equivalenced restricted Hartree–Fock–Roothaan (SERHF) level.[24] Hybrid valence atomic orbitals for each atom were generated from the localized molecular orbitals (LMO) by truncation of the functions on the

(4) (a) Ruedenberg, K. *Rev. Mod. Phys*, **1962**, *34*, 326. (b) Feinberg, M. J.; Ruedenberg, K.; Mehler, E. L. *Adv. Quantum Chem*, **1970**, *5*, 28. (c) Feinberg, M. J.; Ruedenberg, K. *J. Chem. Phys*. **1971**, *54*, 1495. (d) Kutzelnigg, W. *Angew. Chem*. **1973**, *85*, 551; *Angew. Chem., Int. Ed. Engl*, **1973**, *12*, 546. (e) Levine, I. N. *Quantum Chemistry*, 3rd ed.; Allyn and Bacon, Inc.: Boston, 1983; Chapter 13.

(5) (a) Bader, R. F. W.; Chandra, A. K. *Can. J. Chem*. **1968**, *46*, 953. (b) Bader, R. F. W.; Preston, H. J. T. *Int. J. Quantum Chem*. **1969**, *3*, 327.

(6) Savariault, J. M.; Lehmann, M. S. *J. Am. Chem. Soc*. **1980**, *102*, 1298.

(7) (a) Breitenstein, M.; Dannohl, H.; Meyer, H.; Schweig, A.; Seeger, R.; Seeger, U.; Zittlau, W. *Int. Rev. Phys. Chem*. **1983**, *3*, 335. (b) Breitenstein, M.; Dannohl, H.; Meyer, H.; Schweig, A.; Zittlau, W. In *Electron Distributions and the Chemical Bond*; Coppens, P., Hall, M. B., Eds.; Plenum Press: New York, 1982.

(8) Dunitz, J. D.; Seiler, P. *J. Am. Chem. Soc*. **1983**, *105*, 7056.

(9) (a) Duntiz, J. D.; Schweizer, W. B.; Seiler, P. *Helv. Chim. Acta* **1983**, *66*, 123. (b) Seiler, P.; Schweizer, W. B.; Dunitz, J. D. *Acta Crystallogr*. **1984**, *B40*, 319. (c) Hirshfeld, F. L. *Ibid*. **1984**, *B40*, 484. (d) Hirshfeld, F. L. *Ibid*. **1984**, *B40*, 613.

(10) (a) Dunitz, J. D.; Schweizer, W. B.; Seiler, P. *Helv. Chim. Acta* **1983**, *66*, 134. (b) Chakrabartri, P.; Seiler, P.; Dunitz, J. D. *J. Am. Chem. Soc*. **1981**, *103*, 7378.

(11) Also see references cited in ref 8.

(12) Coulson, C. A. *Valence*, 2nd ed.; Oxford University Press: London, 1961, especially pp 81–91.

(13) (a) Bader, R. F. W.; Henneker, W. H.; Cade, P. E. *J. Chem. Phys*. **1967**, *46*, 3341. (b) Bader, R. F. W.; Beddall, P. M. *Ibid*. **1972**, *56*, 3320.

(14) (a) Bader, R. F. W.; Keaveny, I.; Cade, P. E. *J. Chem. Phys*. **1967**, *47*, 3381. (b) Bader, R. F. W.; Bandrauk, A. D. *Ibid*. **1968**, *49*, 1653. (c) Cade, P. E.; Bader, R. F. W.; Henneker, W. H.; Keaveny, I. *Ibid*. **1969**, *50*, 5313.

(15) (a) Bader, R. F. W.; Essen, H. *J. Chem. Phys*. **1984**, *80*, 1943. (b) Bader, R. F. W.; MacDougall, P. J.; Lau, C. D. H. *J. Am. Chem. Soc*. **1984**, *106*, 1594. (c) Bader, R. F. W. *Acc. Chem. Res*. **1985**, *18*, 9. (d) Cremer, D.; Kraka, E. *Angew Chem., Int. Ed. Engl*. **1984**, *23*, 627. (e) Cremer, D.; Kraka, E. *Croat. Chem. Acta* **1984**, *57*, 1259.

(16) The following paper emphasizes orientation effects. Schwarz, W. H. E.; Valtazanos, P.; Ruedenberg, K. *Theor. Chim. Acta* **1985**, *68*, 471.

(17) (a) Dunning, T. H., Jr. *Theor. Chim. Acta* **1970**, *53*, 2823. (b) Huzinaga, S. *Ibid*. **1965**, *42*, 1293.

(18) (a) Dunning, T. H., Jr.; Hay, P. J. In *Methods of Electronic Structure Theory*; Schaefer, H. F., III, Ed.; Plenum Press: New York, 1977; Chapter 1. (b) Dunning, T. H., Jr. *J. Chem. Phys*. **1971**, *55*, 3958.

(19) (a) Herzberg, G. *Molecular Spectra and Molecular Structure I. Spectra of Diatomic Molecules*; D. Van Nostrand Co.: New York, 1966. (b) Page 380 of ref 4e.

(20) Roothaan, C. C. J. *Rev. Mod. Phys*, **1951**, *23*, 69.

(21) (a) Hall, M. B. *Int. J. Quantum Chem*. **1978**, *14*, 613; *Chem. Phys. Lett*. **1979**, *61*, 461; *Int. J. Quantum Chem. Symp*. **1979**, *13S*, 195; *Recent developments and applications of multiconfiguration Hartree-Fock methods*, 1981, NRCC Proceedings No. 10, Dupuis, M., Ed.; p 31. (b) Taylor, T. E.; Hall, M. B. *J. Am. Chem. Soc*. **1980**, *102*, 6136.

(22) Foster, J. M.; Boys, S. F. *Rev. Mod. Phys*. **1960**, *32*, 300.

(23) Newton, M. D.; Switkes, E. *J. Chem. Phys*. **1971**, *54*, 3719.

(24) Guest, M. F.; Saunders, V. R. *Mol. Phys*. **1974**, *28*, 819.

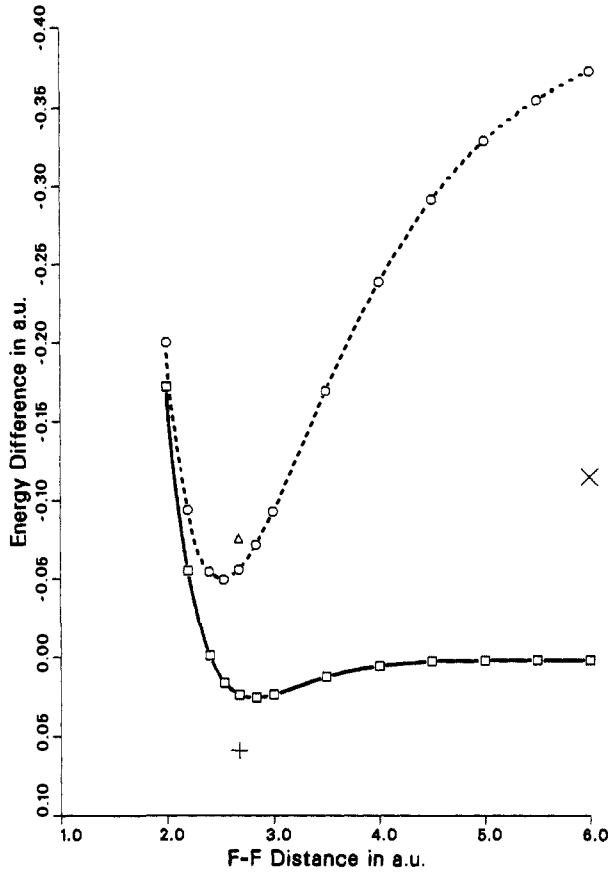

Figure 2. Dissociation curves for F_2 from the single determinant (○) and GMO–CI ($3\sigma_g$, $3\sigma_u$) (□) calculations in the TZP basis relative to two ^2P atoms. Relative energy of the molecule in the TZ basis (△) and experimental value (+) at the experimental R(F–F) = 2.68 au. Relative energy of two valence-state hybrids (×) at R(F–F) = ∞.

other atom.[25] Atomic core orbitals and hybrid atomic valence orbitals were then renormalized and symmetrically orthogonalized with use of the Löwdin procedure.[26] The energy of the resulting hybrid atom was determined. All of the above were performed with a modified ATMOL3 system of programs.[27]

The various wave functions with the appropriate electron occupation numbers were used in the program MOPLOT[28] to generate total electron density maps and bonding orbital and lone-pair orbital electron density maps for the molecule and for the atoms. Density difference maps were generated by subtraction of one total map from another. Individual orbital density difference maps were generated by subtraction of the atomic orbital density map from the molecular orbital density map. All of the above calculations were performed on the Texas A&M University Chemistry Department VAX 11/780 computer.

Maps with contours of constant density difference were plotted on a Xerox 9700 Electronic Printing System with the graphics package called Electronic Printer Image Construction (EPIC) using the program CONTOUR[29] on the Texas A&M University Amdahl 470V/6 and V/7 computers. In the contour line diagrams, solid lines represent positive density difference and dashed lines represent negative difference. The smallest positive and negative contours are ±0.1 electron Å^{-3}, and adjacent contours of the same sign differ by an increment of 0.10 electron Å^{-3} in all maps.

Results and Discussion

Computational Aspects: Polarization Functions and Correlation. In the HFR density maps, all the molecular orbitals are doubly occupied, while in the GMO–CI density maps all are doubly occupied except for the $3\sigma_g$ and $3\sigma_u$ natural orbitals, whose occupation numbers were obtained from the GMO calculation as 1.861 and 0.139, respectively. Shown in Figure 1a is the difference in the electron density of the HFR molecule with and without polarization functions. As can be seen in Figure 2, the HFR molecule in both basis sets is unbound with respect to the dissociated ground-state atoms by 32.8 and 47.5 kcal mol^{-1}, respectively. The addition of polarization functions results in a small change in energy of the molecule, but a large increase in electron density in the internuclear region, consistent with previous findings that the basis set error in molecular densities is pronounced and that polarization functions are important for an adequate representation of the molecular charge density,[7,30] They do not, however, contribute to the ground-state ^2P atomic charge density.

As can be seen in Figure 2, the GMO–CI calculation accounts for a major portion, 68%, of the differential electron correlation. Now the molecule is bound with respect to the dissociated ground-state atoms by 14.9 kcal/mol. The experimental dissociation energy is 37 kcal/mol.[19b] The correlation density, which is the difference in density computed with the GMO–CI wave function and with the HFR wave function, can be seen in Figure 1b and is similar to that found by other researchers for F_2.[7] Electron correlation shifts electron density from the internuclear and lone-pair regions to regions near the nuclei.[7] The addition of electron correlation results in a large change in energy but only a small change in electron density at the bond center.[5a,7,30] Although calculations in larger basis sets or larger CI may modify the actual magnitude of the density shifts, they should not alter the qualitative aspects of our results.

Atom Deformation Densities. Accumulation of electron density in the bonding region between the nuclei and the depletion in the nonbonding region occur in the prototype covalent bonds of the hydrogen molecule and hydrogen molecule ion. H_2 and H_2^+ do not exhibit a separate and significant increase in density in their antibonding region because no lone pairs are present.[5b] Since the ground-state $^1\Sigma_g^+$ of F_2 has a valence configuration of $2\sigma_g^2 2\sigma_u^2 3\sigma_g^2 1\pi_u^4 1\pi_g^4 3\sigma_u^0$ and is usually considered to be covalently σ bonded, we would expect constructive interference along the bond direction.

Substraction of the superposition of two spherically averaged atomic densities from the molecular GMO–CI density results in the standard deformation density for F_2 in Figure 3a. It shows density deficits along the bond axis in both the internuclear bonding region and the lone-pair regions beyond the nuclei and accumulation in the π regions perpendicular to the axis. This result is at variance with our intuition, but it resembles experimental and theoretical maps of the deformation density of covalent bonds between electronegative atoms where the valence shells are more than half filled.[6-11] The problem is that although the analysis of electron difference densities based on a promolecule of spherical atoms is experimentally quite appealing, it may not be the most appropriate reference density for a discussion of the bonding.

Individual F atoms are not spherical; the spherical atom is a convenient reference density but has statistical validity only as a collection of F atoms. Each spherical $2s^22p^5$ F atom in this arbitrary reference is a linear combination of all components of the spectroscopic ^2P ground state of the atom such that the $2p_x$, $2p_y$, and $2p_z$ orbitals are, on the average, each occupied by 5/3 electrons, as in Figure 4a. Only one properly oriented ^2P component, as shown in Figure 4b, contributes significantly to the

(25) (a) A somewhat related method was developed by Newton, Switkes, and Lipscomb (Newton, M. D.; Switkes, E.; Lipscomb, W. N. *J. Chem. Phys.* **1970**, *53*, 2645), who transformed canonical SCF orbitals to "localized" (LMO) form by the Edmiston–Ruedenberg procedure[25b] and then extracted the portion of each LMO belonging to the central atom as the appropriate hybrid. (b) Edmiston, C.; Ruedenberg, K. *Rev. Mod. Phys.* **1963**, *35*, 457.

(26) Lowdin, P.-O. *J. Chem. Phys*, **1950**, *18*, 365.

(27) Hillier, I. H.; Saunders, V. R.; Guest, M. F. *ATMOL3 System*; Chemistry Department, University of Manchester: Manchester, U.K., and SRC Laboratory: Daresbury, U.K.

(28) Lichtenberger, D. L. Ph.D. Dissertation, University of Wisconsin, Madison, WI, 1974. Program available from the Quantum Chemiistry Program Exchange, Indiana University, Bloomington, IN 47401; Program 284.

(29) An in house program that uses CONREC, a special smoothing routine for drawing contours, developed at the National Center for Atmospheric Research (NCAR), Boulder, Co. and adapted for use on the Amdahl 470V/6 by Thomas Reid, Data Processing Center, Texas A&M University.

(30) Hall, M. B. In *Electron Distributions and the Chemical Bond*; Coppens, P., Hall, M. B., Eds.; Plenum Press: New York, 1982; Chapter 4.1.

(31) Ruedenberg, K.; Schmidt, M. W.; Gilbert, M. M.; Elbert, S. T. *Chem. Phys.* **1982**, *71*, 65.

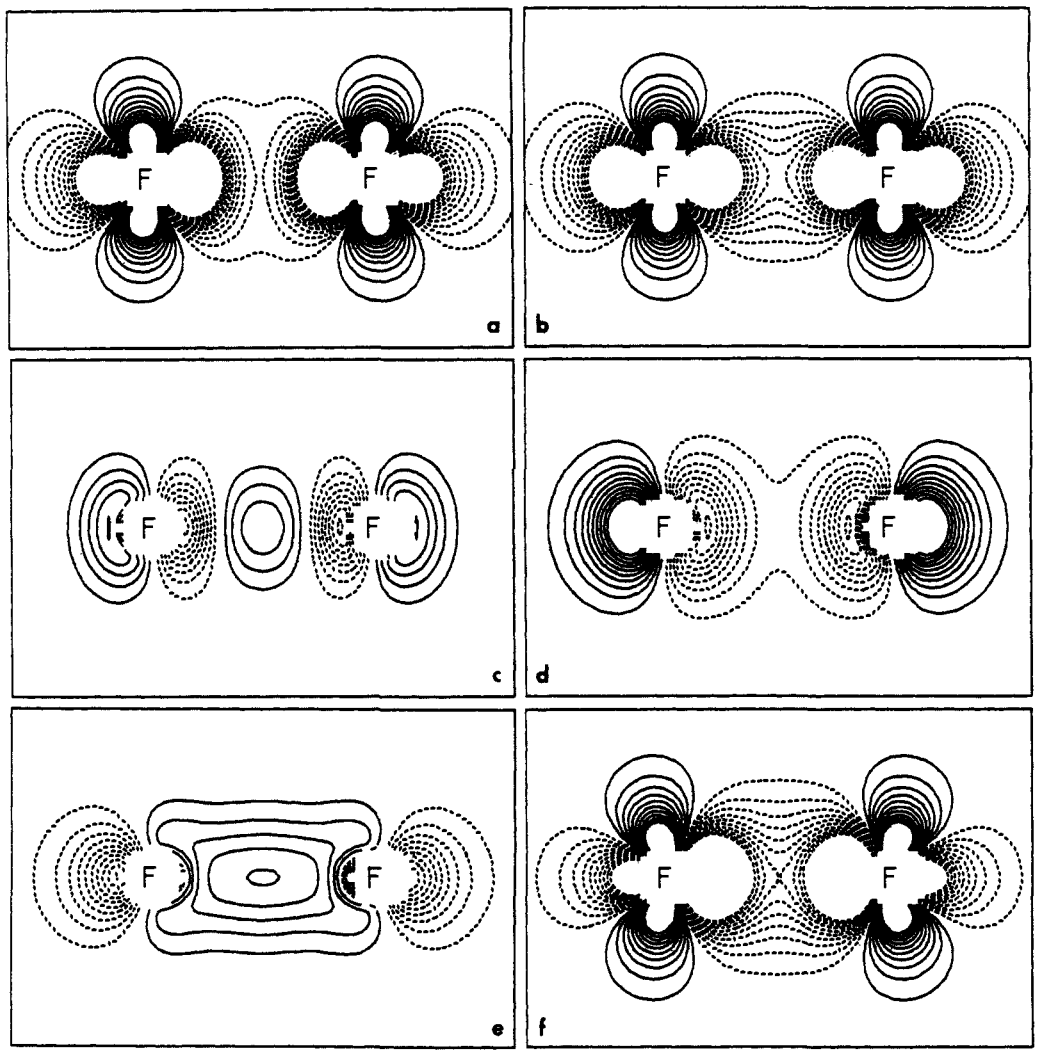

Figure 3. Contour plots of differences in electron density distributions for F_2 from the GMO–CI molecular density: (a) molecule minus spherical atoms; (b) oriented atoms minus spherical atoms; (c) molecule minus oriented atoms; (d) valence-state hybrid atoms minus oriented atoms; (e) molecule minus valence-state hybrid atoms; and (f) valence-state hybrid atoms minus spherical atoms.

ground state of F_2. The other ^2P components occur with very small weights in the ground state of F_2,[31] and contribute predominantly to excited states of F_2, which have configurations $2\sigma_g^2 2\sigma_u^2 3\sigma_g^2 1\pi_u^4 1\pi_g^2 3\sigma_u^2$ ($^1\Sigma^+$, $^3\Sigma^-$, and $^1\Delta$) and $2\sigma_g^2 2\sigma_u^2 3\sigma_g^2 1\pi_u^4 1\pi_g^3 3\sigma_u^1$ ($^1\Pi$ and $^3\Pi$). Inclusion of these other components in the spherical atom results in 1/3 fewer electrons removed per atomic $2p_\pi$ orbital from the doubly occupied molecular $1\pi_u$ and $1\pi_g$ orbitals, resulting in positive deformation densities in the $2p_\pi$ regions at each atom. Compared to the doubly occupied σ bonding molecular orbital, an extra 2/3 electron in each atomic $2p_\sigma$ orbital is subtracted out of the bonding region. This more than compensates for the constructive interference and results in a negative deformation density in that area. Proof that the standard deformation density is dominated by this atomic rearrangement is shown in Figure 3b, where the density of spherical F atoms is subtracted from the density of oriented F atoms, $2p_\sigma^1 2p_\pi^4$. The similarity of a and b in Figure 3 is remarkable.

One component of the ^2P ground state of the F atoms has the same energy as the linear combination of all ^2P components but has a nonspherical, oriented charge distribution with doubly occupied $2p_x$ and $2p_y$ orbitals and a singly occupied $2p_z$ orbital, as shown in Figure 4b. The deformation density which corresponds to the dissociation energy is the molecular density minus that of two F atoms, each being this one component of the ^2P state with the $2p_z$ orbital along the σ direction. This deformation density map, Figure 3c, shows a weak accumulation of charge in the bonding region between the nuclei, deep troughs of density deficit near the nuclei, no change along the π regions, and accumulation

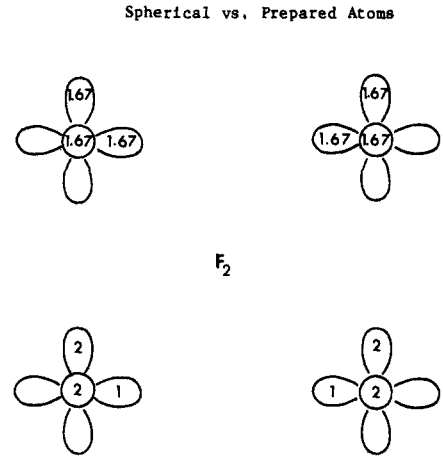

Figure 4. Schematic representation of the atomic orbital occupations and orientations in the promolecule density for F_2: (a) spherical atom (linear combination of all components of the ^2P F ground state); and (b) oriented atom (one component of the ^2P F ground state with the $2P_\sigma$ orbital singly occupied and the $2P_\pi$ orbitals doubly occupied).

of charge in the lone-pair regions beyond the nuclear centers. This deformation density is similar to the near Hartree–Fock density difference by Bader, Henneker, and Cade,[13a] which also used an oriented reference state.

The features in this map correspond to a net bonding density from constructive interference plus lone-pair density from po-

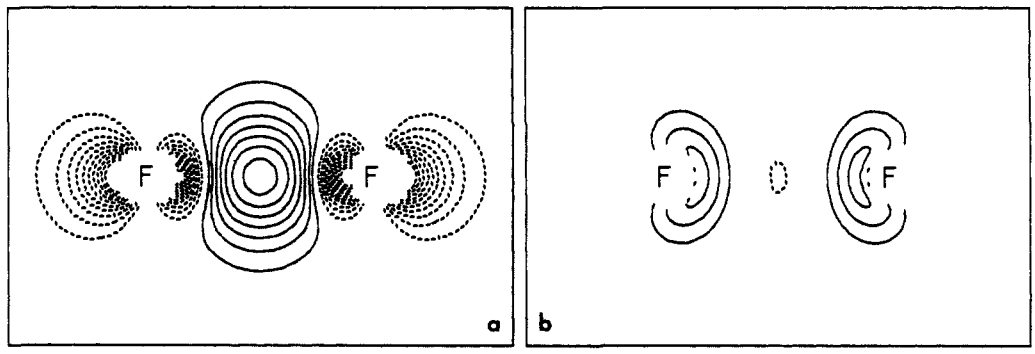

Figure 5. Contour plots of orbital density differences for F_2: (a) localized doubly occupied σ bonding molecular orbital minus singly occupied valence-state σ hybrids; and (b) sum of six localized doubly occupied lone pair orbitals minus six corresponding doubly occupied atomic hybrids.

larization and hybridization. Bader et al.[13] note that the density difference in the lone-pair region exceeds that in the bonding region. Although the calculations suggest that the σ bond is mainly $2p_z$ in character, some hybridization and polarization of the 2s occurs, in part, to move the doubly occupied, nonbonding 2s out of the bonding region. An optimum hybridization would match the lone-pair densities of atoms and molecule, so that we would see the bonding density difference only.

Hybrid Atom Deformation Densities. Our analysis of the LMO's shows the bonding atomic orbital to be 90% $2p_z$, i.e., $sp^{9.3}$, consistent with the results of other hybridization procedures for difluorine.[32] Lennard-Jones has shown that in the absence of other forces, the Pauli exclusion principle will force electrons of like spin confined to a sphere to remain as far apart as possible.[33] This would result in canonical hybrids, in this case, sp^3. Other forces in a molecule reduce the degree of hybridization from that of the canonical hybrids. The optimum hybrids have an intrinsic existence which is dependent on the number of electrons in the valence shell and on the energy difference between the 2s and 2p orbitals.[34] Since the promotion energy of the hybrid atoms is a dominant factor[34] and the average difference in energy of the 2s and 2p orbitals is relatively large,[35] the hybridization is small in difluorine. When hybridization mixes 2s character into the singly occupied $2p_z$ orbital, the doubly occupied 2s loses electron density and the $2p_z$ gains electron density. The mainly 2s lone-pair hybrid points away from the bond center and contains 2 electrons, while the mainly $2p_z$ bond hybrid points toward the bond center and contains only one electron. This hybridization reduces but does not eliminate nonbonded repulsions related to the Pauli exclusion principle. As can be seen in Figure 3d, the density of the hybrid atoms minus that of the oriented atoms, the atom promotion, polarization, and hybridization corresponds to a relatively strong charge displacement to the outside of the F atoms because the resulting hybrids are unequally occupied. Two valence-state F atoms lie about 72 kcal/mol above two ^2P state atoms, but the energy lowering due to bond formation is greater, as can be seen in Figure 2.

If the valence-state F atoms are assumed to be separated atoms with the pairing of their electrons and polarization preserved as they were in the molecule, then covalent bond formation between the valence-state F atoms results in the change in density shown in Figure 3e, which was calculated as the density of the GMO–CI molecule minus the density of the hybrid atoms. This map reveals not only a stronger accumulation of charge in the internuclear region than in the map where the ground-state oriented ^2P F atoms were subtracted but also density deficits in the nonbonding regions beyond the nuclear centers. Thus the deformation density for F_2 in Figure 3c has been partitioned into two parts, d plus e in Figure 3.

Figure 5a shows the bonding orbital electron density difference, i.e., the difference in density between the localized 2-electron bonding molecular orbital and two singly occupied valence-state σ hybrid atomic orbitals. The sum of the lone-pair orbital density differences, shown in Figure 5b, is almost featureless. Thus, the primary features of the total density difference in Figure 3e are reduced to that of the 2-electron bonding molecular orbital density difference (Figure 5a).

In the bonding orbital density difference, the pattern of the accumulation of charge in the internuclear region and the deficit along the bond axis beyond the nuclear centers is what one would expect for a simple 2-electron covalent σ bond made from p type orbitals. Since the deformation density must integrate to zero, the density buildup between the nuclei must be compensated by loss elsewhere. The bonding molecular orbital density,

$$\Psi^2 = (1/(2 + 2S))(\psi_a^2 + \psi_b^2 + 2\psi_a\psi_b) \quad (1)$$

where $S = \int \psi_a\psi_b \, d\tau$ is the overlap integral, exceeds the sum of the two isolated atomic bonding orbitals densities,

$$\psi_a^2 + \psi_b^2 \quad (2)$$

in the overlap region between the nuclei where $\psi_a\psi_b$ is large. In the nonbonding regions the bonding molecular orbital density is less than the densities of the atomic bonding orbitals due to the $(2 + 2S)$ factor in the denominator.

The preparation of atoms for bonding by orientation of the atoms and then atomic polarization, promotion, and hybridization prior to molecular formation results in the change in density shown in Figure 3f, which was calculated as the difference in density between the hybrid atoms and the spherically averaged atoms. Thus, the standard deformation density for F_2, Figure 3a, has partitioned into two parts, f plus e in Figure 3. The former corresponds to the change in density in preparation for bonding (orientation of ground-state ^2P atoms, polarization, promotion, and hybridization) and the latter corresponds to the change in density due to covalent bond formation (constructive interference between optimum valence-state hybrids).

Conclusion

Since the observable is the total density of the molecule, all partitioning schemes are arbitrary. The subtraction of any promolecule is useful only if it reveals features not visible in the total density. For practical reasons most experimentalists choose to substract a promolecule made from spherical atoms. However, as we have shown, accumulation of density in certain covalent bonds, especially bonds between electronegative atoms, can appear weak because of the choice of a spherical-atom promolecule. Orientation of the atoms in the promolecule improves the situation and is particularly important because it has a dramatic effect on the density difference but does not change the energy.[16] Additional features beyond the orientation effect can be revealed by using the chemical concept of a valence-state atom. Using these "prepared for bonding" atoms, one can reduce the complex difference density of F_2 to a difference density of a two-electron bond.

(32) Foster, J. P.; Weinhold, F. *J. Am. Chem. Soc.* **1980**, *102*, 7211 and references therein.

(33) Lennard-Jones, J. E. *J. Chem. Phys.* **1952**, *20*, 1024.

(34) (a) Hall, M. B. *J. Am. Chem. Soc.* **1978**, *100*, 6333. (b) Hall, M. B. *Inorg. Chem.* **1978**, *17*, 2261.

(35) Murrell, J. N.; Kettle, S. F. A.; Tedder, J. M. *Valence Theory*, 2nd ed.; John Wiley & Sons: New York, 1970; p 34.

Thus, if one views the bond formation in two steps, (1) creation of valence-state atoms then (2) bond formation, the accumulation of density in the bond due to (2) is quite large even for F_2. In contrast to the F–F bond, the standard deformation densities of C–C and C–H bonds show quite large accumulations of density, since the density of the usual spherical atom reference is much closer to that of the valence state for C and H than it is for F.

Acknowledgment. The authors gratefully acknowledge the support of the National Science Foundation (Grant No. CHE 83-09936).

Registry No. F_2, 7782-41-4.

Inverted Tricoordinate Carbon[1]

Koop Lammertsma

Contribution from the Department of Chemistry, University of Alabama at Birmingham, University Station, Birmingham, Alabama 35294. *Received November 7, 1985*

Abstract: Eleven four-membered ring structures (C_4, C_4H^+, $C_4H_2^{2+}$, C_3BH, $C_3BH_2^+$, $C_2B_2H_2$, C_3Be, C_3BeH^+, C_2BBeH, C_2Be_2, and B_4H_2) are discussed in terms of stability properties associated with inverted tricoordinate carbons. These minimum energy structures have short distances between the bridgehead carbons, averaging 1.484 Å (6-31G*), and short ring bonds, with average values for C–C, C–B, and C–Be bonds of 1.396, 1.487, and 1.576 Å, respectively. The stabilities of these molecules result from four-center, two-electron (aromatic) π bonding and a nonbonding σ HOMO between the bridgehead carbons. The Mulliken overlap population between these carbons ranges from −0.236 for $C_4H_2^{2+}$ to +0.495 for C_2Be_2. While there is no bridgehead–bridgehead bonding in $C_4H_2^{2+}$, there is in C_2Be_2. The beryllium isomers possess ionic character.

Strained hydrocarbons are of fundamental importance for understanding carbon–carbon bonding properties.[2] A particularly interesting feature is revealed in the series of saturated hydrocarbons: ethane,[3] cyclopropane,[3] bicyclo[1.1.0]butane (**1**),[4] and [1.1.1]propellane (**2**).[4g,5,6] In this series the geometry of the sp^3

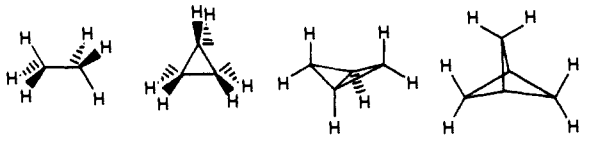

1 **2**

Table I. 6-31G* Energies, Structural Parameters, and Mulliken Overlap Population Analysis for the Four-Membered Ring Structures **5–15**

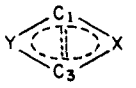

5, X = Y = C
6, X = CH^+; Y = C
7, X = Y = CH^+
8, X = BH, Y = C
9, X = BH; Y = CH^+
10, X = Y = BH
11, X = Be; Y = C
12, X = Be; Y = CH^+
13, X = Be; Y = BH
14, X = Y = Be
15, X = Y = BH; C = B

compound	energy	geometry $r(C_1–C_3)$	geometry r(C–X), r(C–Y)	overlap population
5,[a] C_4	−151.145 98	1.457	1.425	−0.063
6,[a] C_4H^+	−151.456 93	1.520	1.352, 1.472	−0.013
7,[a] $C_4H_2^{2+}$	−151.539 98	1.593	1.386	−0.236
8, C_3BH	−138.653 29	1.462	1.479, 1.418	0.138
9, $C_3BH_2^+$	−139.012 20	1.529	1.526, 1.345	0.060
10, $C_2B_2H_2$	−126.155 41	1.470	1.470	0.330
11, C_3Be	−127.983 66	1.418	1.563, 1.421	0.219
12, C_3BeH^+	−128.393 88	1.484	1.619, 1.345	0.107
13, C_2BBeH	−115.478 31	1.445	1.558, 1.473	0.389
14, C_2Be_2	−104.791 29	1.458	1.564	0.495
15 B_4H_2	−99.721 64	1.690[b]	1.604[b]	0.306

[a] Reference 8. [b] The respective r(B–B) bonds are given.

hybridized carbons in ethane is inverted by the subsequent replacement of vicinal hydrogens for CH_2 groups with no significant effect on the (6-31G*) C–C distance. Moreover, while the carbons in ethane are bonded, this is not the case in [1.1.1]propellane.[5e] The intriguing bonding phenomena of the latter compound with its inverted tetracoordinate carbons are well documented,[5,7]

How are the bonding properties of unsatured hydrocarbons affected when the geometry of the neighboring tricoordinate carbons is inverted? There are two general deformations possible for sp^2 hybridized carbons, the out-of-plane and the in-plane deformations. The out-of-plane deformation has been subject to

(1) Lammertsma, K. Presented at the 190th National Meeting of the American Chemical Society, Chicago, IL, Sept 1985; paper ORG 233.

(2) Greenberg, A.; Liebman, J. F. *Strained Organic Molecules*; Academic: New York, 1978. Ginsburg, D. *Propellanes*; Verlag Chemie: Weinheim, Germany, 1975.

(3) For theoretical data see: (a) *The Carbegie-Mellon Quantum Chemistry Archive*, Whiteside, A., Frisch, M. J., Pople, J. A., Eds.; 3rd ed.; Carnegie-Mellon University: Pittsburgh, PA, 1983. (b) Bader, R. F. W.; Slee, T. S.; Cremer, D.; Kraka, E. *J. Am. Chem. Soc.* **1983**, *105*, 5061.

(4) (a) Disch, R. L.; Schulman, J. M.; Sabio, M. L. *J. Am. Chem. Soc.* **1985**, *107*, 1904. (b) Pacansky, J.; Yoshimine, M. *J. Phys. Chem.* **1985**, *89*, 1880. (c) Richtsmeier, S. C.; Gassman, P. G.; Dixon, D. A. *J. Org. Chem.* **1985**, *50*, 311. (d) Eckert-Maksic, M.; Maksic, Z. B.; Gleiter, R. *Theor. Chim. Acta* **1984**, *66*, 193. (e) Osawa, E.; Szalontai, G.; Tsurumoto, A. *J. Chem. Soc., Perkin Trans. 2* **1983**, 1209. (f) Gassman, P. G.; Greenlee, M. L.; Dixon, D. A.; Richtsmeier, S.; Gougoutas, J. Z. *J. Am. Chem. Soc.* **1983**, *105*, 5865. (g) Wiberg, K. B. *Ibid.* **1983**, *105*, 1227. (h) Gassman, P. G.; Yamaguchi, R. *Tetrahedron* **1982**, *38*, 1113. (i) Paddon-Row, M. N.; Houk, K. N.; Dowd, P.; Garner, P.; Schappert, R. *Tetrahedron Lett.* **1981**, 4799. (j) Skancke, P. N. *THEOCHEM* **1982**, *3*, 255. (k) Bader, R. F. W.; Tang, T. H.; Tal, Y.; Biegler-Koenig, F. W. *J. Am. Chem. Soc.* **1982**, *104*, 940, 946. (l) Chakrabarti, P.; Seiler, P.; Dunitz, J. D.; Schlutter, A.-D.; Szeimies, G. *Ibid.* **1981**, *103*, 7378. (m) Adam, W.; Oppenlaender, T.; Zang, G. *Ibid.* **1985**, *107*, 3921. (n) Becknell, A. F.; Berson, J. A.; Srinivasan, R. *Ibid* **1985**, *107* 1076. (o) Sponsler, M. B.; Dougherty, D. A. *J. Org. Chem.* **1984**, *49*, 4978. (p) Chang, M. H.; Jain, R.; Dougherty, D. A. *J. Am. Chem. Soc.* **1984**, *106*, 4211. (q) Gassman, P. G.; Carroll, G. T. *J. Org. Chem.* **1984** *49*, 2074. (r) Chang, M. H.; Dougherty, D. A. *J. Am. Chem. Soc.* **1982**, *104*, 2333.

(5) (a) Wiberg, K. B.; Walker, F. H. *J. Am. Chem. Soc.* **1982**, *104*, 5239. (b) Semmler, K.;Szeimies, G.; Belzner, J. *Ibid.* **1985**, *107*, 6410. (c) Wiberg, K. B. *Tetrhedron Lett.* **1985**, 599. (d) Vuckovic, D. L.; Vujisic, L. *Croat. Chem. Acta* **1984**, *57*, 801. (e) Jackson, J. E.; Allen, L. C. *J. Am. Chem. Soc.* **1984**, *106*, 591. (f) Michl, J.; Radziszewski, G. J.; Downing, J. W.; Wiberg, K. B.; Walker, F. H.; Miller, R. D.; Kovacic, P.; Jawdosiuk, M.; Bonacic-Koutecky, V. *Pure Apl. Chem.* **1983**, *55*, 315. (g) Bader, R. F. W.; Tang, T. H.; Tal, Y.; Biegler-Koenig, F. W. *Ibid.* **1982**, *104*, 940. (h) Wiberg, K. B.; Wendoloski, J. J. *Ibid.* **1982**, 104, 5679. (i) Newton, M. D.; Schulman, J. M. *Ibid.* **1972**, *94*, 773. Stohrer, W.-D.; Hoffmann, R. *Ibid.* **1972**, *94*, 779.

(6) (a) Wiberg, K. B.; Dailey, W. P.; Walker, F. H.; Waddell, S. T.; Crocker, L. S.; Newton, M. *J. Am. Chem. Soc.* **1985**, *107*, 7247. (b) Honegger, E.; Huber, H.; Heilbronner, E.; Dailey, W. P.; Wiberg, K. B. *Ibid.* **1985**, *107*, 7172. (c) Hedberg, L.; Hedberg, K. *Ibid.* **1985**, *107*, 7257.

(7) Wiberg, K. B. *Acc. Chem. Res.* **1984**, *17*, 379.

0002-7863/86/1508-5127$01.50/0